Heliyon 9 (2023) e12817

Contents lists available at ScienceDirect

Heliyon

journal homepage: www.cell.com/heliyon

Research article

Epoxidation of *Argemone mexicana* oil with peroxyacetic acid formed in-situ using sulfated tin (IV) oxide catalyst: Characterization; kinetic and thermodynamic analysis

Fekadu Ashine [a], Subramanian Balakrishnan [a], Zebene Kiflie [b], Belachew Zegale Tizazu [a,*]

[a] Department of Chemical Engineering, Addis Ababa Science and Technology University, Addis Ababa, 16417, Addis Ababa, Ethiopia
[b] School of Chemical and Bio-Engineering, Addis Ababa Institute of Technology, Addis Ababa, Ethiopia

ARTICLE INFO

Keywords:
Argemone mexicana oil
Epoxidation
Peroxy acetic acid
Sulfated tin (IV) oxide
Kinetic model

ABSTRACT

In this study, sulfated tin (IV) oxide solid acid catalyst was prepared for the epoxidation of *Argemone mexicana* oil (AMO) with peroxyacetic acid formed in-situ. The catalyst was synthesized using the chemical co-precipitation method and characterized. The effects of various epoxidation parameters on ethylenic double bond conversion (%) and oxygen ring content were analyzed. The maximum ethylenic double bond conversion of 95.5% and epoxy oxygen content of 6.25 was found at the molar ratio of AMO to 30% of H_2O_2 = 1:2.5, molar ratio of AMO to acetic acid = 1:1.5, catalyst concentration = 12.5%, and reaction temperature = 70 °C at reaction time = 6 h. The kinetic and thermodynamic features of the epoxidation of AMO were also analyzed with appropriate models. The results of the kinetic study of the epoxidation reaction followed pseudo first order with the activation energy = 0.47.03 kJ/mol. Moreover, the thermodynamic constants of epoxidation of AMO were found as ΔH = 44.18 kJ/mol, ΔS = −137.91 $Jmol^{-1}k^{-1}$) and ΔG = 91.12 kJ/mol. The epoxidized product of AMO was further analyzed using FTIR, ^{1}H NMR, and ^{13}C NMR. The results of these analyses confirmed the successful conversion of the ethylenic double bond in the AMO to EAMO.

1. Introduction

Due to rising environmental concerns and challenges in satisfying future demand, the demand for renewable raw materials to replace petroleum oil-based products is significantly increasing [1]. It is one of the green synthesis choices that can help with long-term sustainability [2]. Vegetable oils (VOs), which currently account for the majority of renewable feedstocks used to make bio-based products, might be a viable alternative for the production of bio-based products [3]. Hence, the use of VOs as a potential feedstock for a variety of functional materials and their applications in a variety of sectors has recently gained greater attention. Long-chain fatty acid triglyceride esters are utilized as a trustworthy starting material for the production of a wide range of bio-based fuels and chemical products [4]. However, the degree of unsaturation present in the oil causes rancidity, stability, lubricity, compatibility, and chemical degradation problems which limit their use as petroleum oil alternatives [5–7]. As a result, the scientific community is paying more attention to the functionalization of VOs via epoxidation. Non-edible vegetable oils, such as castor oil [8], jatropha oil [9], Cynara

* Corresponding author.
E-mail address: belachew.zegale@aastu.edu.et (B.Z. Tizazu).

https://doi.org/10.1016/j.heliyon.2023.e12817
Received 13 September 2022; Received in revised form 29 December 2022; Accepted 3 January 2023
Available online 9 January 2023

cardunculus seed oil [1], cottonseed oil [10], Mahua oil [11], etc., have emerged as possible alternatives to address low-cost material demands without competing with food crops. Argemone mexicana oil is an ideal choice for making epoxidized oil, which is a renewable alternative for a variety of applications. This is because of their inherent biodegradability, availability, sustainability, non-toxicity, and ease of chemical modification of VO, as well as environmental concerns and limited supply of petroleum [12].

Argemone mexicana oil (AMO) is a non-edible seed oil derived from Mexican prickly poppy seeds, an annual growing weed plant in the Papaveraceae family [13]. It is primarily composed of triglycerides of unsaturated long-chain fatty acids with high linoleic acid (36.6–61.4%) and oleic acid (18.5–40%), which are playing an important role in the epoxidation process [14]. Epoxidation is the most common VOs modification method for functionalizing ethylenic double bonds in VOs and converting them into the highly reactive epoxy group. They are adaptable building blocks for making bio-based products like plasticizers, lubricants, PVC stabilizers, and surface coating formulations [8,15,16]. This can also result in a variety of stable products with a highly reactive oxirane ring that aids in the investigation of a variety of chemical reactions [17]. Generally, the epoxidation of vegetable oils is performed with peroxy acid formed in situ since H_2O_2 has very low solubility in vegetable oils [11,17–19]. Acetic acid is more selective than formic acid, because the side reaction of peracetic acid decomposition is lower than performic acid, and the side reaction of ring opening is lower than with formic acid [20]. Consequently, epoxidized oil has increased viscosity, lubricity, oxidative stability, compatibility, and thus making the materials more susceptible to microbial degradation, all of which are crucial characteristics of epoxy products [3,12,21,22]. Various studies have been reported on the epoxidation of VOs with peroxy acids formed in situ utilizing homogenous catalysts, acidic ion exchange resins (AIER), or biocatalysts for epoxy formation with a wide range of applications, particularly for PVC plasticizers, and lubricants [10,15,21,23]. During epoxidation employing peroxy carboxylic acid as an oxidizer catalyzed by a homogenous catalyst, mainly sulphuric acid, produces commercially viable epoxidized oils [19]. [24] used peracetic acid to make epoxy canola oil employing sulphuric acid catalyst to convert ethylenic unsaturation to oxirane (81%) at 7 h. However, they can cause a variety of undesirable side reactions as well as corrosion problems [25,26]. Moreover, enzymes are also used as effective biocatalysts for the epoxidation of VOs in recent years [27]. used immobilized lipase as a biocatalyst for epoxidation of genetically modified high oleic acid soybean oil with or without free fatty acid and toluene, resulting in the epoxide conversion of 95% at 35 °C. The chemo-enzyme epoxidation of different VOs such as soybean oil [28], Sapindus Mukorossi seed oil [29], and Karanja oil [30] with other bio-catalysts such as Novozym 435, have been reported using hydrogen peroxide as an oxidant. But, the chemo-enzyme epoxidation of VOs is strongly influenced by hydrogen peroxide concentration as well as high temperatures, resulting in enzyme deactivation [26]. The employment of heterogeneous catalysts, including AIER for epoxidation of VOs, would be more advantageous in terms of separation ease, reusability, eco-friendly, and cost effectiveness [31]. [32] have reported on Karanja oil (iodine value, 89 g/100g) epoxidation with peracetic acid catalyzed by Amberlite IR-120 catalyst. The researchers have studied the effects of stirring speed, molar ratio of hydrogen peroxide to ethylenic double bond in the oil, molar ratio of acetic acid to ethylenic double bond in the oil, temperature, and catalyst loading for the epoxidation process [24]. also described on epoxidation of canola oil with in situ generated peroxy acetic acid using Amberlist IR120H resin as a catalyst and obtained oxirane oxygen content of 90% at 7 h.

Metal oxide solid acid catalysts are used in a variety of organic synthesis processes, including aromatic nitration, esterification, transesterification, and epoxidation [33]. Thus, heterogeneous metal oxide catalysts are preferred to circumvent the limits of the aforementioned catalysts [3]. There have been a few reports on the epoxidation of soybean oil, canola oil, podocarpus falcatus seed oil, methyl oleate, and sunflower oil using heterogonous metal oxides as a catalyst such as sulfonated –ion exchange resins [32], sulfonated- SnO_2 [3], solid sulfonated silica acid [34], Ti–SiO_2 [18], Alumina [35], tungsten [36], respectively [34]. used sulfonated silica solid acid catalyst for epoxidation of podocarpus falcatus seed oil with hydrogen peroxide as an oxidizer. The maximal ethylenic conversion to oxirane was reported to be 84.75% under optimal conditions ethylenic double bond to H_2O_2 molar ratio of (2.5:1), catalyst loading (5%), temperature (70 °C), and time (4 h). Sulfated tin (IV) oxide is also classified as a super solid acid because of its high surface acidity and is employed in the majority of acid-catalyzed processes like esterification and transesterification [19]. [37] reported that a sulfate-doped metal oxide surface can function as a solid acid and an oxidative catalyst [3]. also used sulfated tin (IV) oxide to epoxide unsaturation in canola oil using peroxyacetic acid produced in situ from H_2O_2 and acetic acid. They reported a maximum epoxide conversion of 100% at optimum epoxidation conditions [33]. studied solid acid sulfated – Zirconia for effective epoxidation of castor oil. Because certain sulfate-doped metal oxides such as SnO_2, ZrO_2, TiO_2, and Al_2O_3 have both Lewis and Brønsted acid sites derived from metal oxides and sulfates doped on the surface of metal oxides, they have been widely used as a solid acid in organic chemical modifications. Furthermore, as compared to metal oxides without sulfate, they produce super acid materials with high surface acidity and significantly larger surface areas [38]. As a result of their exceptional catalytic activity, they have attracted a lot of attention and are frequently utilized as a solid acid catalyst for a range of organic modifications. As far as the authors knowledge, sulfated tin (IV) oxide solid acid-catalyzed epoxidation of Argemone mexicana oil with peroxy acetic acid formed in situ has not been reported elsewhere.

Various researchers have studied kinetic modelling strategies to estimate kinetic constants for the epoxidation of cottonseed oil by Prileschajew method [39]. have used a semi-batch reactor to study kinetic modelling for the epoxidation of cottonseed oil with performic acid by Prileschajew method. The results of their study showed that the reaction enthalpy of epoxidation and ring opening was −230 kJ/mol and −90 kJ/mol, respectively with initial reaction conditions of 50–70 °C, an organic phase 30–40%, formic acid 0.02–0.05 mol/min and time 25–50 min [40]. used a kinetic model under adiabatic conditions to investigate the variables affecting the risk of thermal runaway for the epoxidation of cottonseed oil. It has been noted that adiabatic temperature rise and time to maximum rate were sensitive to the content of acetic acid and hydrogen peroxide [41]. estimated the kinetic constants for the epoxidation of cottonseed oil by peroxyacetic acid using a batch reactor. The authors developed a kinetic modelling technique to predict kinetic constants for the ring opening reaction involving water, acetic acid, and peracetic acid. They reported that ring opening by acetic and peracetic acids more quickly than water and hydrogen peroxide.

Therefore, this study aimed to synthesize and characterize sulfated–tin (IV) oxide solid acid as a heterogeneous catalyst for AMO epoxidation with peroxy acetic acid formed in situ. The influences of various AMO epoxidation parameters (viz. molar ratio of the ethylenic double bond in the AMO to H_2O_2, molar ratio of the ethylenic double bond in the AMO to acetic acid, catalyst concentration, and reaction temperature) were investigated. The physicochemical characteristics of AMO and its epoxidized oil (EAMO) were also examined. Moreover, a kinetic model for AMO epoxidation was analyzed to proceed to the acceptable degree of double bond conversion.

2. Materials and methods

2.1. Materials

Hydrogen peroxide (30%), glacial acetic acid (99.5%), ammonia solution (30%), iodine crystals, HBr solution (48%), sodium thiosulphate, anhydrous sodium sulfate, sulphuric acid (98%), ethyl acetate, Stannous chloride dihydrate ($SnCl_2.2H_2O$, 97%) and chloroform (99%) were purchased from Sigma-Aldrich (Germany). The other chemicals and reagents utilized in this experiment were analytical grade.

2.2. Oil extraction

Oil was extracted from Argemone mexicana seed (AMS), collected from Addis Ababa, Ethiopia, using the soxhlet method with chloroform as the solvent. The maximum oil yield was achieved at a temperature near the boiling point of the corresponding solvent [42]. After the complete extraction process, the extracted oil was separated from the solvent using a rotary evaporator and vacuum pump at 70 °C. Prior to the epoxidation process, the obtained oil was refined and stored at −4 °C for further use in the epoxidation process.

2.3. Synthesis of sulfated tin (IV) oxide solid acid catalyst

In this study, sulfate group-doped tin (IV) oxide solid acid catalyst for the AMO epoxidation was prepared by applying the chemical co-precipitation method [3,43–45]. 75 g of $SnCl_2.2H_2O$ (97%) and 1.5 L deionized water were mixed with a continuous stir followed by a dropwise addition of 30% of aqueous ammonia solution to maintain the desired pH of ~9.0. At room temperature, a white tin hydroxide ($Sn(OH)_4$) powder gel was precipitated after 6 h. The resultant gel was filtered using Whatman's filter paper and rinsed with distilled water until a neutral solution. The gel was then oven-dried at 100 °C for overnight. Then, 20 g of the obtained gel powder was impregnated with 300 mL of 1 M sulphuric acid solution for 1 h. Further acid-treated tin hydroxide powder gel was oven-dried at 100 °C for 12 h. Both oven-dried tin hydroxide and its related acid-treated gel powder were calcined at 500 °C for 4 h. Finally, several surface characterizations were performed on the resulting pure tin (IV) oxide and sulfate group doped-tin (IV) oxide catalysts using FTIR, XRD, BET/BJH, DSC, TGA, SEM-EDX methods, thereby understanding catalyst activity.

2.4. Sulfated tin (IV) oxide solid acid catalyst characterization

FTIR (Thermo fisher FTIR spectrometer-Nicolet iS50), at 4 cm^{-1} resolution with KBr as a background matrix in the range of 4000–400 cm^{-1}, were used to determine the formation of pure tin (IV) oxide and its sulfated solid acid catalyst. In FTIR analysis, 5 mg of both resultant catalysts and 95 mg of KBr crystal were thoroughly mixed, grounded into a fine powder, and then pelletized using a hydraulic press at 10 tons. Thus, the functional groups present on the catalyst surfaces were identified using this technique.

XRD was also conducted on a diffractometer with Ni-filtered CuKα radiation at $\lambda = 0.154$ nm in the 2θ range of 10–80° and thus the crystal structure and sizes of both catalysts were determined. Accordingly, the mean crystal sizes of the catalysts were calculated using the Debye Scherer equation as indicated in eq. (1).

$$D = \frac{0.9\lambda}{\beta \cos\theta} \tag{1}$$

where D –denotes the average diameter of crystalline size (nm), λ –denotes the wavelength of CuKα radiation at 0.154 nm, β –denotes full width at half maximum intensity (FWHM) in radian, and θ –denotes for Bragg angle (o).

Brunauer - Emmett-Teller (BET) devices based on adsorption and desorption of N_2 gas isotherms via Quantachrome Nova 2200e Surface Area analyzer (USA) was used to characterize surface areas of both resultant catalysts (pure tin (IV) oxide and it's sulfate doped - tin (IV) oxide solid acid catalyst). The specific surface areas of both catalysts were determined from a nitrogen adsorption study conducted at a low temperature (−196.15 °C) using the high vacuum conventional volumetric glass system and were evacuated at 250 °C for 2 h before exposure to nitrogen gas at −196.15 °C under reduced pressure (10^{-5}tor). Besides, the micrometric Pore Size analyzer Barret –Joyner Halenda (BJH) technique was used to evaluate the pore volume and average pore diameter of the obtained catalysts.

Thermal gravimetric analysis (TGA) was also employed to study the thermal stability of the resultant catalysts under the temperature range of 25–750 °C using TA instruments with SDT Q600 under nitrogen flow in which weight losses were evaluated. Then, further confirmation analysis was conducted using differential scanning calorimetry (DSC).

2.5. Epoxidation of Argemone mexicana oil (AMO)

All epoxidation processes were conducted in 500 mL three-necked round bottom flasks with a magnetic stirrer and placed in the hot plate's temperature-controlled water bath. One side of the flask was inserted with a thermometer and used to measure reaction temperature, while the other middle neck of the flask was fitted to a water-cooled reflux condenser. Primarily, the required amount of AMO was mixed with acetic acid and sulfated tin (IV) oxide solid acid catalyst at 30 °C at a stirring speed of 1000 rpm. Then, 30% of hydrogen peroxide solution was added dropwise to the reaction mixture in the first 30 min. The reaction time recording was begun once this oxidizer was completely added to the reaction mixture. The influence of reaction conditions, such as molar ratio of the ethylenic double bond in the oil to H_2O_2 and acetic acid, catalyst concentration, and the reaction temperature were studied. Upon completion of the epoxidation process, catalysts were removed by filtration. Before analysis, the reaction products were collected and ethyl acetate (50 mL) was used to separate the aqueous and organic oil layers periodically, then washed with both $NaHCO_3$ (5%) solution and distilled water until pH ~7, and the trace amount of water and other impurities was absorbed with anhydrous Na_2SO_4. Finally, the resultant epoxy products were separated from ethyl acetate using a rotatory evaporator. The epoxy oxygen content was analyzed using AOCS Cd 9–57 methods in which 0.1 N hydrobromic solution in acetic acid (glacial) was used as a titrate (as per eq. (2).), and the ethylenic double bond conversion into an epoxy group was determined in terms of iodine value (IV). The amount of double bonds in the oil is closely related to the iodine value (IV), which is an indicator of the overall unsaturation in the AMO. As a result, IV was determined to find out the quantity of double bonds in the oil. Hence, the ethylenic double bond conversion was investigated in terms of the iodine (IV) value measurements, using the AOCS Cd 1–25 method according to eq. (3). Further epoxidized oil formation confirmation analyses were conducted using FTIR, ^{1}H NMR, and ^{13}C NMR methods.

$$OOC = \frac{0.1M\ x\ 1.6\ x\ (B - V)}{weight\ of\ sample\ (g)} \tag{2}$$

where, OOC stands for oxirane oxygen content (%), B stands for volume of hydrobromic acid solution used to titrate a blank, and V stands for volume of hydrobromic acid solution used to titrate the test sample.

$$IV = \frac{\mathrm{M}\ x\ 12.69\ x\ (B - S)}{weight\ of\ sample\ (g)} \tag{3}$$

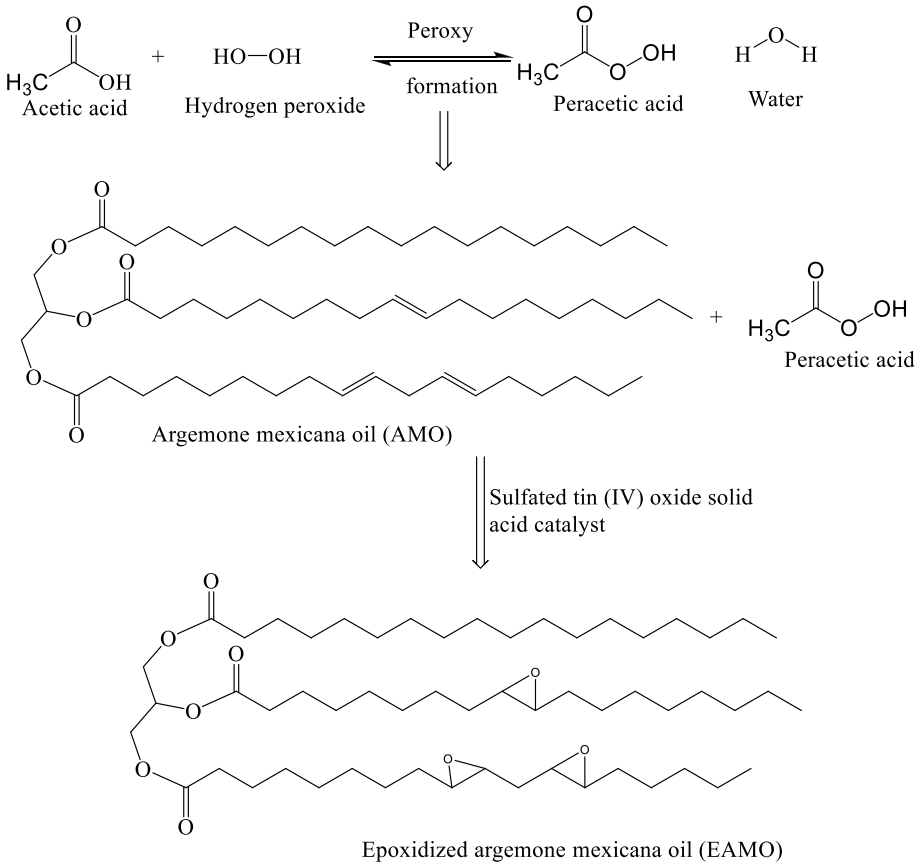

Scheme 1. Schematic illustration of EAMO formation.

where IV stands for iodine value, M stands for molarity of sodium thiosulphate, B stands for mL of sodium thiosulphate used to titrate a blank, and S stands for the mL of sodium thiosulphate used to titrate the test sample. In addition, the ethylenic DB conversion in the AMO to the epoxy group was determined using eq. (4) [46].

$$Ethylenic\ DB\ conversion\ (\%) = \frac{IV_0 - IV}{IV} x100 \tag{4}$$

where, IV denotes the iodine value of the AMO before epoxidation in g I_2/100g of oil, and IV is the iodine value of the EAMO in g I_2/100g.

To better understand the influences of epoxidation reaction conditions on epoxide conversion, the different experimental trials were conducted following the one-variable-at-a-time method. All epoxidation experiments were done with a constant 50 mL of AMO and 1000 rpm mixing speed for 6 h. In this study, the effect of sulfated – tin (IV) oxide solid acid catalyst loading varied from 5 to 15% with corresponding to the weight of AMO on the ethylenic double bond conversion and epoxy oxygen ring content, while other reaction parameters such as the molar ratio of an ethylenic double bond in the AMO to 30% of H_2O_2 1:3, the ethylenic double bond in the AMO to acetic acid ratio 1:2, and reaction temperature 70 °C were taken from the literature [3]. The effects of the ratio of the ethylenic double bond in the AMO to hydrogen peroxide (30%) on the ethylenic double bond (DB) conversion and epoxy oxygen content were investigated by varying the range from 1:1 to 1:4 at fixed optimal catalyst loading value, the molar ratio of the ethylenic double bond the AMO to acetic acid 1:2, and reaction temperature (70 °C). The effect of the ratio of the ethylenic double bond in the AMO to acetic acid was varied from 0.5 to 2.5 at fixed other epoxidation parameters. The reaction temperature was also altered from 50 to 80 °C to investigate its impact on an ethylenic double bond conversion and thus epoxy oxygen content. The overall AMO epoxidation process is shown in Scheme 1.

2.6. Physicochemical characteristics of epoxidized oil (EAMO)

The physicochemical characteristics of the epoxidized product (EAMO) such as density, kinematic viscosity at 40 °C (mm^2/s), kinematic viscosity at 100 °C (mm^2/s), viscosity index, flash point (°C), epoxy oxygen ring content (%), and iodine values (g I_2/100g of the AMO) were examined using established methods. Using a Rheometer (MCR 102, USA) instrument, the dynamic viscosity of AMO and its epoxidized oil (EAMO) were measured as a function of temperature ranging from 20 to 100 °C at a constant shear rate of 50 per second. Furthermore, the kinematic viscosity and viscosity index of both AMO and its epoxidized oil was determined using the determined dynamic viscosity value based on the ASTMD2270 standard table. The viscosity index (VI) of EAMO was calculated using eq. (5). The flash point of AMO and its epoxidized oil were also examined. According to a standard procedure, the iodine values (IV) of both samples were tested using eq. (3).

$$VI_x = \frac{\gamma_A - \gamma_x}{\gamma_A - \gamma_B} x100\ at\ 40\ ^o c\ x100 \tag{5}$$

Where VI_x denotes viscosity index of the AMO/EAMO, γ_x denotes kinematic viscosity of Epoxidized oil (EAMO) at 40 °C, γ_A and γ_B denotes kinematic viscosity of oil A and B at 40 °C are used as reference oil taken from ASTM-D2270-10 table for γ_x at 100 °C.

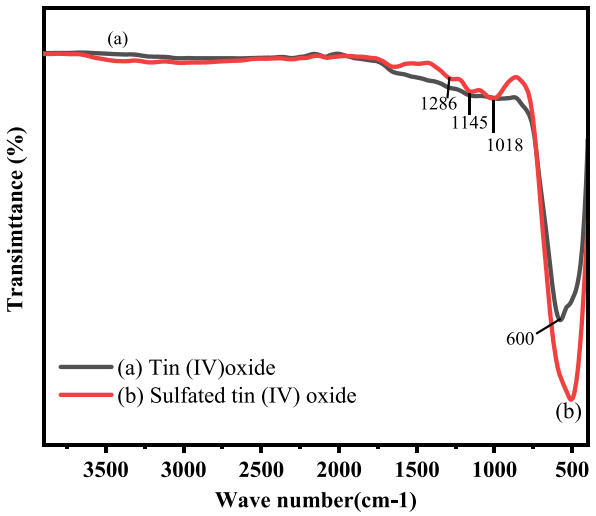

Fig. 1. FTIR spectral analysis for tin (IV) oxide (a), and sulfated tin (IV) oxide (b).

3. Results and discussion

3.1. Sulfated tin (IV) oxide solid acid catalyst characterization

FTIR spectra of obtained pure and sulfated tin (IV) oxide catalysts are presented in Fig. 1a and b. The characteristic peaks at 600 cm^{-1} show the existence of O–Sn–O stretching. This revealed the complete conversion of tin (IV) hydroxide gel into SnO_2 when calcined at 500 °C for 4 h. Similarly, bands at 1286, 1145, and 1018 cm^{-1} were observed in the spectra after sulfation of tin (IV) hydroxide gel with 1 M H_2SO_4, indicating symmetric and asymmetric stretching frequencies of the sulfated group (S═O) and confirming a bidentate chelation (linkage) mode between sulfate group and tin (IV) oxide. This further indicates the formation of sulfate doped – tin (IV) oxide as a solid acid catalyst after being calcined at 500 °C for 4 h. Because of the existence of sulfate doped on the surface of tin (IV) oxide catalyst, robust acidic properties can be recognized [38]. Thus, improving the properties of sulfate doped tin (IV) oxide catalyst is important for promoting the epoxidation of AMO with peroxyacetic acid generated in situ. Similar research works were reported by Refs. [43–45].

The XRD spectra of attained pure tin (IV) oxide and sulfated tin (IV) oxide solid acid catalyst are illustrated in Fig. 2a. The major absorption peaks at 26.63°, 33.90°, 37.99°, 51.81°, 54.80°, 61.91°, 64.78°, 65.99°, 71.75° are related to diffraction from planes (110), (101), (200), (211), (220) of tin (IV) oxide particles. This shows the complete conversion of tin (IV) hydroxide gel into pure tin (IV) oxide by calcination at 500 °C for 4 h, and thus confirms the tetragonal crystal phase. Similarly, after sulfation of this gel with 1 M H_2SO_4 treatment, XRD peaks at 26.63°, 33.93°, 37.98°, 51.84°, 54.76°, 61.91°, 64.82°, 65.98°, and 78.73° are related to the above-mentioned diffraction planes. This indicates that the sulfate group doped on the catalyst's surface did not cause any crystalline changes. This is supported via the DCS plot in Fig. 2b, confirming that the prepared catalysts have a single phase. However, sulfation of tin (IV) oxide reduces the crystalline size of the obtained tin (IV) oxide thereby increasing the surface area of the catalyst which in turn enhances its catalytic activity. The mean crystalline sizes of pure tin (IV) oxide and tin (IV) oxide doped with the sulfate group were determined using the Debye Scherrer eq. (1) based on XRD peak width measurements. Accordingly, the calculated mean crystalline size of tin (IV) oxide and sulfated tin (IV) oxide solid acid catalyst was determined to be 35.62 nm and 16.64 nm, respectively. This smaller crystal size of the sulfate group-linked tin (IV) oxide catalyst is related to the addition of sulfate ions. This could be due to sulfate chelation on the catalyst surface, which prevents the tin (IV) oxide particles from coagulating during the calcination process at 500 °C for 4 h. As a result, the surface area of the sulfated tin (IV) oxide solid acid catalyst increased and thus improved its catalytic performance for the AMO epoxidation process. This demonstrates that sulphuric acid treatment has a significant impact on reducing crystalline size, increasing surface area, and so improves the catalytic activity of sulfated tin (IV) oxide for epoxidation. Comparable results were reported in the literature [3,45].

Catalyst surface area is one of the critical parameters that have a significant influence on catalytic activity, and thus epoxide conversion. Brunauer – Emmett – Teller (BET) was employed to analyze the surface area of each prepared catalyst while Barret –Joyner Halenda (BJH) method was used to characterize pore volume and average diameters. As indicated in Table 1 the BET surface areas of Tin (IV) oxide and sulfate group linked tin (IV) oxide were 14.84 m^2/g and 60.61 m^2/g, respectively. The development of sulfate linkage with tin (IV) oxide gives its increased surface area for the sulfate group linked tin (IV) oxide solid acid catalyst. The deposition of sulfates on the surface of tin (IV) oxide increased its pore volume from 0.06 to 0.13 cm^3/g and caused an increased in the average pore diameter from 10.97 to 11.20 nm, according to the BJH pore size distribution result. Sulfation of tin (IV) oxide enhanced pore volume and is anticipated to boost epoxide output [12,38].

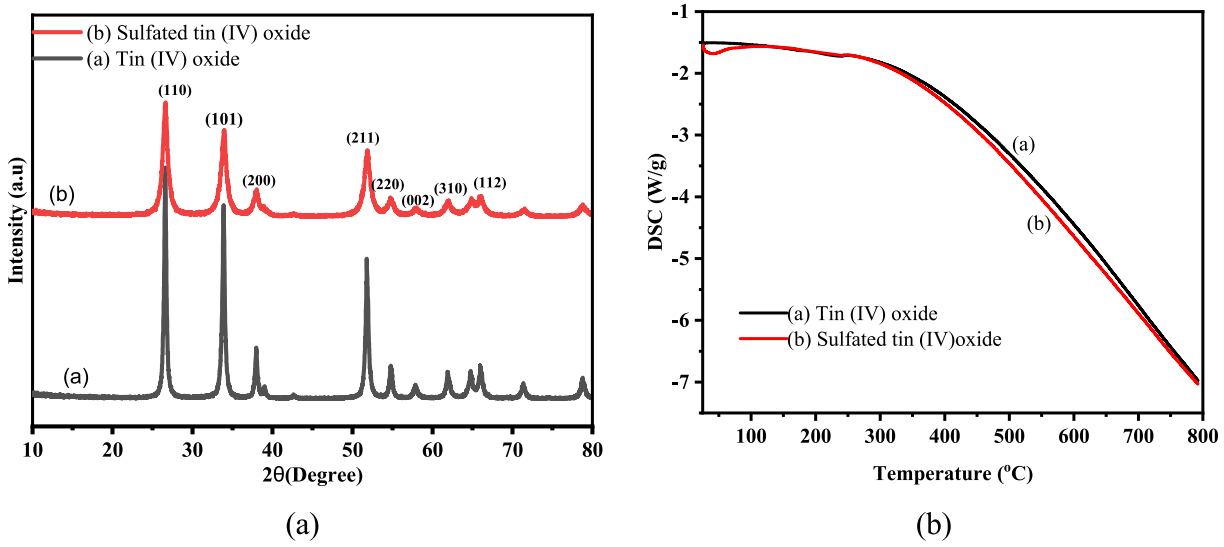

Fig. 2. XRD spectrum pattern of tin (IV) oxide and sulfated tin (IV) oxide (a), and DSC plot of tin (IV) oxide and sulfated tin (IV) oxide (b).

Table 1
BET/BJH results of tin (IV) oxide and sulfate group doped tin (IV) oxide at 500 °C.

Catalyst	Surface area (m^2/g)	Pore volume (cc/g)	Average pore diameter (nm)
Tin (IV) oxide	14.84	0.06	10.97
Sulfated–tin (IV) oxide	60.61	0.13	11.20

The thermal analyses of pure tin (IV) oxide and sulfated tin (IV) oxide after calcination at 500 °C are displayed in Fig. 3a and b. The weight loss of both catalysts was determined in the temperature ranges of 25–800 °C. Tin (IV) oxide was determined to be quite stable up to 800 °C, and the weight loss percentage change was found to be insignificant. Up to 600 °C, sulfated tin (IV) oxide was similar stability with very little weight loss, but after 600 °C, the weight loss increased due to the evolution of the sulfate group from the catalyst surface. Sulfated tin (IV) oxide loses weight when heated to 800 °C compared to pure tin (IV) oxide [3,38].

The surface morphology of both tin (IV) oxide and sulfated tin (IV) oxide catalysts was characterized by SEM analysis. As indicated in Fig. 4a and b, the surface morphology of both catalysts has no significant change after the impregnation of sulfate ions. Sulfation of the catalyst improved the catalytic oxidative activity of tin (IV) oxide surface as compared to non-sulfated metal oxide. Thus, sulfation is the key to boosting the conversion of Argemone Mexicana oil to its epoxidized oil [12,33,43].

3.2. *Effects of AMO epoxidation parameters*

The effect of catalyst concentration on AMO epoxidation is shown in Fig. 5a. In this study, the influence of sulfated tin (IV) oxide solid acid catalyst on the course of AMO epoxidation was evaluated. It was investigated by varying the amounts of the catalyst 5, 7.5, 10, and 15% of the corresponding weight of oil keeping the ratio of the ethylenic double bond in the oil to acetic acid and 30% H_2O_2 as 1:3:2 3. All epoxidation reactions were examined at a constant agitation speed of 1000 rpm at 70 °C. As illustrated in Fig. 5a, the ethylenic double bond (DB) conversion in the AMO to its epoxidized oil gradually increased with an increase in catalyst concentration up to 12.5% due to an increment in the active sites of the catalyst. The maximum double bond conversion of 95.05% and related epoxy oxygen content of 6.25 was achieved after 6 h. However, more upsurge in sulfated tin (IV) oxide catalyst concentration resulted in considerably the same conversion or less. This might be an increased rate of oxygen ring cleavage beyond the maximum value of the catalyst external surface active sites content during epoxidation [8]. In the current investigation, a sulfated tin (IV) oxide solid acid catalyst concentration of 12.5% was shown to be the best value for AMO epoxidation. The results of the study showed that pure tin (IV) oxide calcined at 500 °C has no substantial double bond conversion of AMO into an epoxy group under these experimental conditions [3].

Fig. 5b shows the effect of hydrogen peroxide (30%) on the course of AMO epoxidation at a catalyst concentration of 12.5%, temperature of 70 °C, and the molar ratio of the ethylenic double bond in the AMO to acetic acid 1:2. Hydrogen peroxide has a significant influence on in situ epoxidation [47]. Thus, the ratio of an ethylenic double bond in oil to H_2O_2 (30%) was varied at 1:1, 1:1.5, 1:2, 1:2.5, 1:3, 1:3.5, and 1:4 to study its influence on the in situ epoxidation of ethylenic double bond conversion in the AMO. As shown in Fig. 5b the rate of ethylenic double bond conversion increased with increasing the molar ratio of the ethylenic double bond in the AMO to H_2O_2 (30%). The molar ratio of the ethylenic double bond in AMO to hydrogen peroxide of 1:2.5 resulted in the maximum ethylenic double bond conversion of 95.5% with the highest epoxy oxygen content of 6.25. As the ethylenic double bond in the AMO to hydrogen peroxide (30%) beyond 1:2.5, the ethylenic double bond conversion declined. This is due to an excess supply of 30% of H_2O_2 can cause an upsurge in the degradation rate of oxirane oxygen content [25].

The effect of the ratio of the ethylenic double bond in the AMO to acetic acid (varied at 1:0.5, 1:1, 1:1.5, 1:2, 1:2.5, 1:3) on the in situ epoxidation is shown in Fig. 5c. Though carboxylic acid such as acetic acid acts as a good oxygen carrier during the AMO

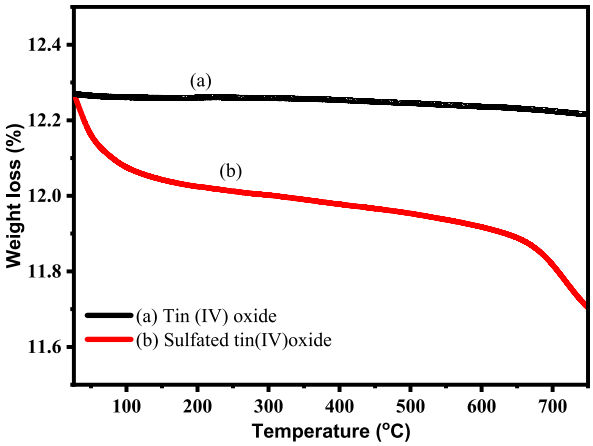

Fig. 3. TGA analysis of Tin (IV) oxide (a) and Sulfated tin (IV) oxide (b).

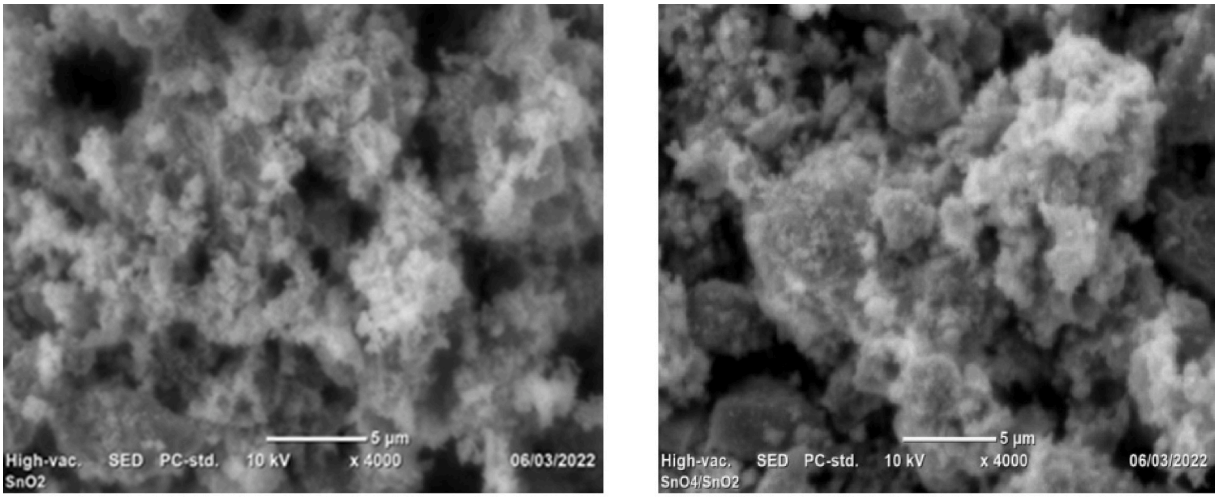

Fig. 4. SEM images of tin (IV) oxide (a) and sulfated tin (IV) oxide (b).

epoxidation, it is the main contributor to the degradation of the oxirane oxygen ring formed [1,21]. It was revealed that the epoxide conversion rate improved with an increase in acetic acid concentration, but further addition resulted in oxygen ring degradation. Thus, the molar ratio of the ethylenic double bond in the AMO to acetic acid was found to be 1:1.5. Under this condition, the maximum ethylenic double bond conversion of 95% and the epoxy oxygen content of 6.25 were obtained after 6 h. Beyond this acetic acid value, the epoxy oxygen content was decreased due to epoxy oxygen ring cleavage owing to the higher acetic acid content.

Fig. 5d shows the effect of epoxidation temperature (varied at 313, 328, 343, and 358 k) on the development of in situ epoxidation, while other epoxidation parameters (viz. molar ratio of the ethylenic double bond in the AMO to 30% H_2O_2 of 1:2.5, molar ratio of the ethylenic double bond in the AMO to acetic acid of 1:1.5, and catalyst concentration 12.5%) were kept constant. As shown in Fig. 5d, an increase in temperature up to 358 k increased the rate of the ethylenic double bond conversion. However, after 6 h, the rate of epoxy formation was found to be slightly constant for 343 K and 358 K.

3.3. Reusability of sulfated tin (IV) oxide solid acid catalyst on AMO epoxidation

Fig. 6 reveals the reusability of sulfate group-doped tin (IV) oxide solid acid on AMO epoxidation was evaluated for four consecutive epoxidation processes under optimized experimental conditions. After the epoxidation reaction, the catalyst was separated and carefully washed, and then refluxed with ethyl acetate to remove reaction products that had formed on the catalyst's surface. Then it was dried overnight in the oven at 100 °C. The in situ epoxidation was carried out at optimal reaction parameters of molar ratio of the ethylenic double bond in oil: H_2O_2: acetic acid 1:2.5:1.5, employing regenerated sulfate chelated tin (IV) oxide solid acid catalyst 12.5% at 343 K for 6 h. The results of the study showed that repeated washing with ethyl acetate leads to the separation difficulty of oil remnants from the pores of the catalyst which poisons catalyst active sites. This causes a gradual loss of catalytic activity after three repeated cycles, and thus lowers ethylenic double bond conversion. It is revealed that oil interaction with catalyst active sites was limited as the number of repeated cycles increased thereby resulting in the lower double bond conversion of AMO.

3.4. Kinetic and thermodynamic analysis of in situ epoxidation of AMO

To explore the reaction mechanism of the AMO epoxidation process catalyzed by sulfated tin (IV) oxide solid acid, experimental runs were conducted at 313, 328, 343, and 358 K to analyze the kinetics and thermodynamics of in situ epoxidation of AMO. The process of epoxidation of AMO is essentially a heterogeneous reaction. To explain the heterogeneous catalytic epoxidation process, the Langmuir – Hinshelwood – Hougen – Watson (LHHW) kinetic expression was suggested. Thus, the reaction that takes place on the catalyst's active sites is principally regulated by three reaction steps: (1) the adsorption of reactants, (2) the surface reaction between adsorbed reactants on the active sites of the catalyst, and (3) desorption of products. However, the in situ epoxidation principally depends on two key reaction steps (i.e. peroxyacetic acid formation and epoxidation steps) since desorption of the product on the catalyst surface is assumed to be weak. In the presence of sulfate group doped tin (IV) oxide solid acid catalyst, epoxidation of AMO with peroxy acetic acid produced in situ from H_2O_2 and CH_3COOH is as in eq. (6):

$$\text{I. } H_2O_2(l) + CH_3COOH(l) \overset{K_1}{\rightleftharpoons} CH_3COOOH(l) + H_2O(l) \tag{6}$$

Assuming that the adsorption of AMO and peracetic acid on catalyst active sites is a mild reaction. Then, the surface reaction

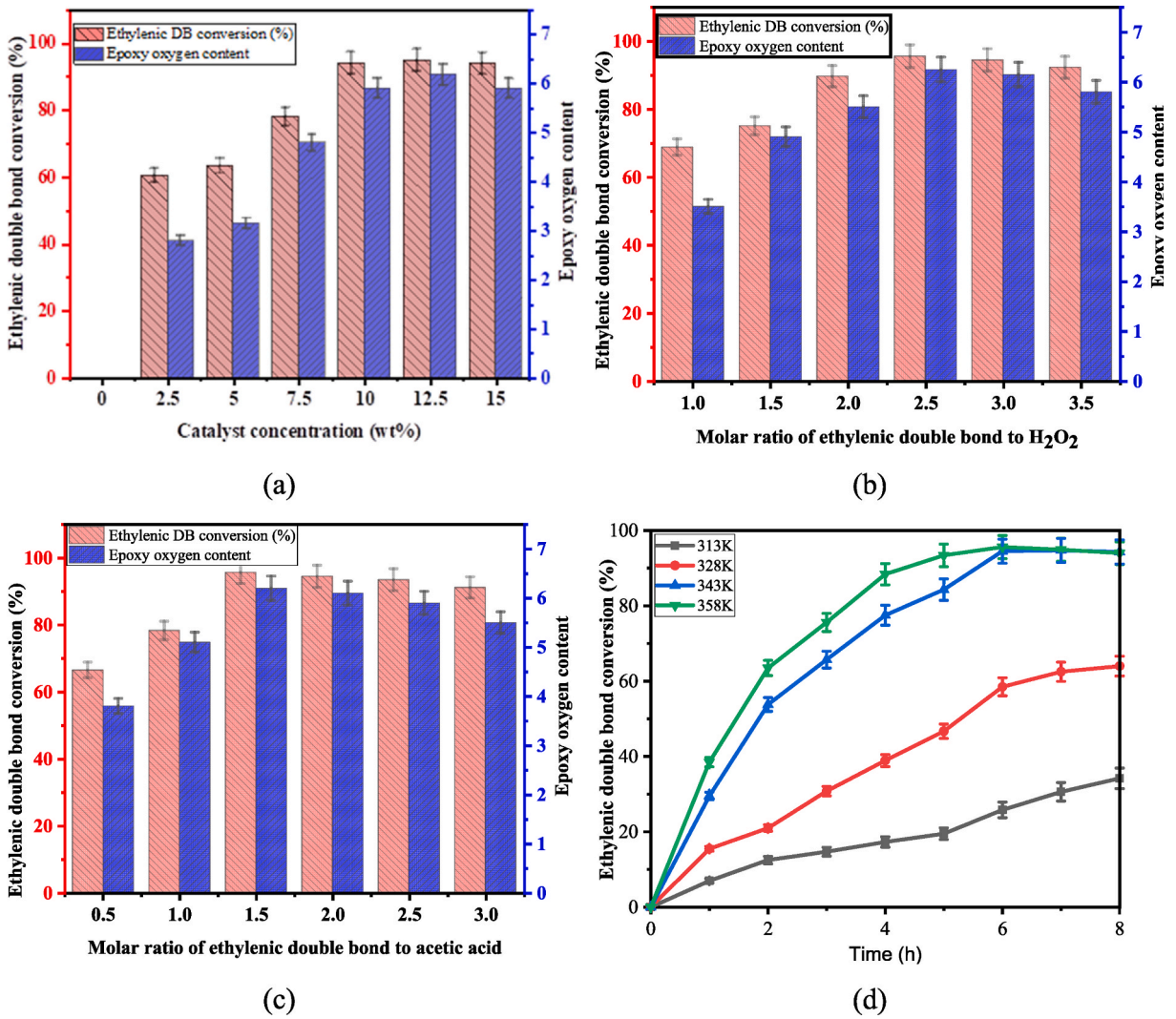

Fig. 5. The effect of catalyst concentration (a), molar ratio of ethylenic double in the AMO to H_2O_2 (b), molar ratio of ethylenic double in the AMO to acetic acid (c), and temperature on the AMO epoxidation (d).

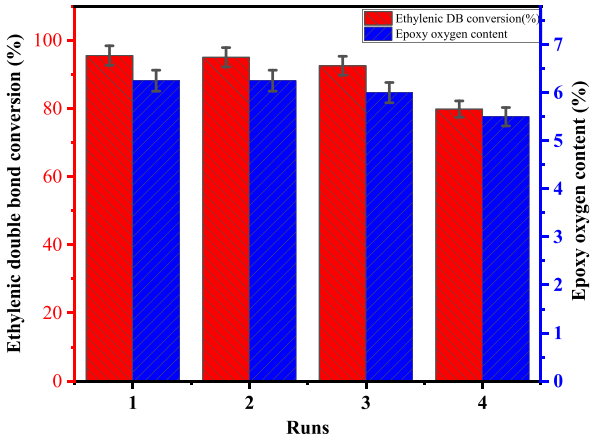

Fig. 6. Reusability of sulfated tin (IV) oxide solid acid catalyst on AMO epoxidation.

between AMO and PAA indicates the formation of epoxidized Argemone mexicana oil (EAMO) and is written as in eq. (7):

$$\text{II. } AMO + PAA + C \overset{K_2}{\rightleftharpoons} EAMO - C \tag{7}$$

The desorption of EAMO is given by eq. (8):

$$\text{III. } EAMO - C \overset{K_3}{\rightleftharpoons} EAMO + C \tag{8}$$

where AMO is Argemone mexicana oil, EAMO is epoxidized argemone mexicana oil, C is sulfated tin (IV) oxide solid acid catalyst, and PAA is peracetic acid.

The kinetic analysis for the epoxidation of AMO was conducted on the basis of the subsequent assumptions.

(I) The rate-controlling step (the slowest step) is considered to be the epoxidation AMO (eq. (7)) whereas peracetic acid formation (eq. (6)) is a rapid and simultaneous step which does not considered a rate-controlling step. Thus, the overall rate equation of epoxidation of AMO considering the epoxidation surface reaction on active sites of catalyst is a rate-determining step is shown in eq. (9):

$$-r_{AMO} = \frac{-dC_{AMO}}{dt} = k^{'} C_{AMO} C_{PAA} \tag{9}$$

(II) Since an excess peracetic acid was used for epoxidation, t can be assumed that peracetic acid content is constant during the epoxidation reaction (i. e. $C_{PAA,o} = C_{PAA}$). Moreover, the epoxidation of AMO is assumed to be a pseudo-first-order reaction. Thus, the rate equation is written as in eq. (10):

$$\frac{-dC_{AMO}}{dt} = kC_{AMO} \tag{10}$$

where, $k = k' C_{PAA}$

Thus, eq. (10) in terms of fractional conversion (X_{AMO}) of oil can be rewritten as in eq. (11):

$$\frac{-dC_{AMO,o}(1 - X_{AMO})}{dt} = kC_{AMO,o}(1 - X_{AMO}) \tag{11}$$

Since, $C_{AMO} = C_{AMO}(1 - X_{AMO})$

Where, $C_{AMO,\,o}$ denotes the initial concentration of ethylenic double bond in the AMO.

$$\frac{-dX_{AMO}}{dt} = k(1 - X_{AMO}) \tag{12}$$

The rate equation can be stated as follows after integrating eq. (12) at $X_{AMO} = 0$, $t = 0$ and $X = X_{AMO}$ at $t = t$.

$$\int_{o}^{X_{AMO}} \frac{-dX_{AMO}}{1 - X_{AMO}} = k \int_{0}^{t} dt \tag{13}$$

Then, after integration of eq. (13), the final rate equation can be written as in eq. (14):

$$-\ln(1 - X_{AMO}) = kt \tag{14}$$

As a result, the experimental data were fitted with linear regression, and the epoxidation rate constants (K) at various temperatures were determined using the slope of $-ln(1 - X_{AMO})$ vs. time plot and tabulated in Table 2. As shown in Table 2, the rate constant (K) values increased with the corresponding reaction temperature increment, revealing that the reaction was pseudo-first-order with respect to AMO.

Arrhenius equation ($k = A^{Ea/RT}$) was utilized to compute the activation energy of AMO epoxidation using the slope of –lnk vs. (1/T, k^{-1}) plot, and is presented in Fig. 7. Therefore, according to the Arrhenius equation plot, the resultant activation energy obtained was 47.03 kJ/mol. This value confirmed that the chemical reaction utilizing sulfate -doped tin (IV) oxide solid acid catalyst was kinetically controlled.

Table 2
Rate constant (k) values for epoxidation of AMO at various temperature.

T (K)	1/T (K^{-1})	k (min^{-1})	–lnk
313	0.003195	0.0490	3.0169
328	0.003049	0.1168	2.1473
343	0.002915	0.3804	0.9665
358	0.002793	0.4054	0.9029

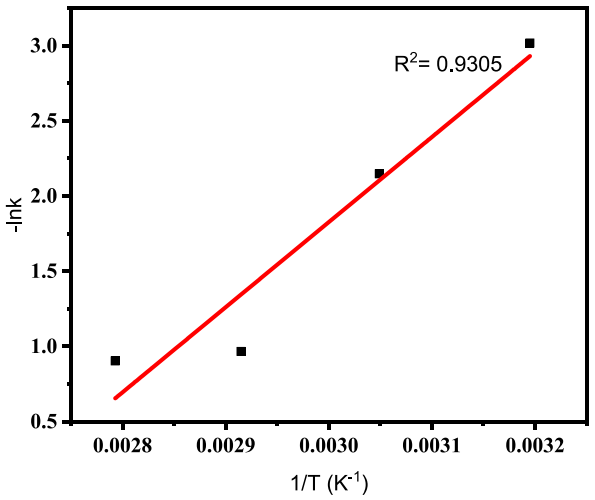

Fig. 7. Plot of –lnk vs 1/T.

The main thermodynamic parameters analyzed under the present study (viz. Gibb's free energy (ΔG), enthalpy (ΔH), and entropy (ΔS)) can be determined using eqs. (15)–(15)–(17)(15)–(17):

$$\Delta H = E_a - RT \tag{15}$$

$$K = \frac{RT}{Nh} e^{\Delta S / R} e \tag{16}$$

$$\Delta G = \Delta H - T\Delta S \tag{17}$$

Using eqs. (15)–(15)–(17)(15)–(17), thermodynamic parameters of epoxidation of AMO using sulfate -doped tin (IV) oxide solid acid catalyst were found to be $\Delta H = 44.18$ kJ/mol, $\Delta S = -137.91$ Jmol^{-1}k^{-1}, and $\Delta G = 91.12$ kJ/mol and tabulated in Table 3. The ΔH value determined was the enthalpy of activation for the epoxidation process. The positive values of ΔH indicate that the energy input (heat) from an external source is required to raise the energy level and transform the reactants to their transition states. Thus, the positive value of enthalpy of activation reveals that the epoxidation process is endothermic in nature. Similar results were reported in various literature [48–52]. The negative value of entropy revealed that the epoxide product is more stable as compared to the AMO. The positive value of Gibb's free energy also showed that the epoxidation of AMO is a non-spontaneous process which is also confirmed by the positive value of enthalpy. The present study is in reasonable agreement with the prior reports, which revealed comparable observations of activation energy of 44.85 kJ/mol for epoxidation of soybean oil and 44.65 kJ/mol for palm oleic acid [17,19].

3.5. FTIR analysis of epoxidized oil (EAMO) formation

Fig. 8a and b shows the FTIR results of AMO and its epoxidized oil (EAMO). It was revealed that the removal of ethylenic double bonds in the AMO and the formation of its epoxidized product (EAMO) by their absorption peaks. The bending and stretching vibration of the ethylenic double bond (=C–H of unsaturated fatty acids) in the AMO is visible in bands at 3008 cm^{-1} and 721 cm^{-1}. However, removing these bands from AMO revealed that the oil has been completely converted to its epoxidized form (EAMO). This was further corroborated by the presence of a new band at 825 cm^{-1}, which was not observed in the AMO, showing that an epoxy oxygen ring (C–O – C) has been formed in the epoxidized oil (EAMO). This matches the appearance of an epoxy oxygen ring in the 785–880 cm^{-1} absorption peak range [17]. The absence of a broad proton signal of the –OH group in epoxidized oil indicates that no major side reactions occurred during in situ epoxidations of AMO with sulfated tin (IV) oxide soil acid catalyst.

Table 3
Thermodynamic constants for epoxidation of AMO using sulfated tin (IV) oxide solid acid catalyst.

T (K)	1/T x 10^{-3} (K^{-1})	–lnk	E_a (kJmol^{-1})	ΔH (kJmol^{-1})	ΔS (Jmol^{-1}K^{-1})	ΔG (kJmol^{-1})	R^2
313	3.195	3.0169	47.03	44.18	−137.12	91.26	0.9305
328	3.049	2.1473					
343	2.915	0.9665					
358	2.793	0.9029					

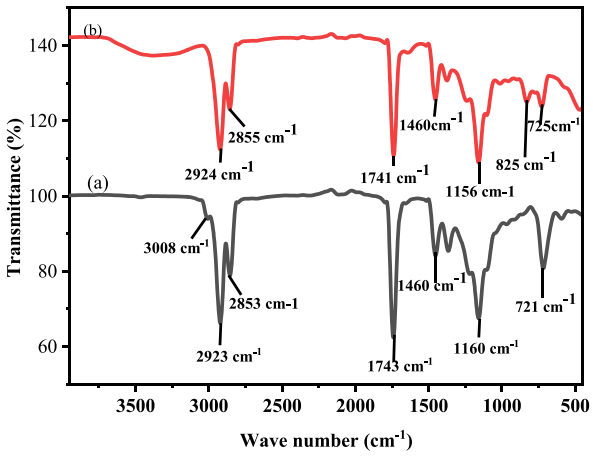

Fig. 8. FTIR spectra of AMO (a) and EAMO (b).

3.6. *^{1}H NMR and ^{13}C NMR analysis of epoxidized oil (EAMO) formation*

Nuclear magnetic resonance spectroscopy (NMR) was used to better understand the synthesis of epoxidized oil (EAMO). This also signifies the ablation of the ethylenic double bond in the AMO and the appearance of an epoxy oxygen ring in the final epoxy product during in situ technique. In Fig. 9a ^{1}H NMR spectra shows the presence of the ethylenic double bond (-C = C-) in the AMO at a chemical shift of 5.3 ppm. However, these ethylenic double bonds in this oil have been vanished in the epoxidized product (EAMO) as shown in Fig. 9b. Furthermore, the existence of new oxirane oxygen ring bands in the epoxy product at 2.7–3.3 ppm and 1.5–1.87 ppm, confirming the conversion of ethylenic double in the AMO to EAMO by in situ epoxidation using sulfate group doped tin (IV) oxide solid acid catalyst.

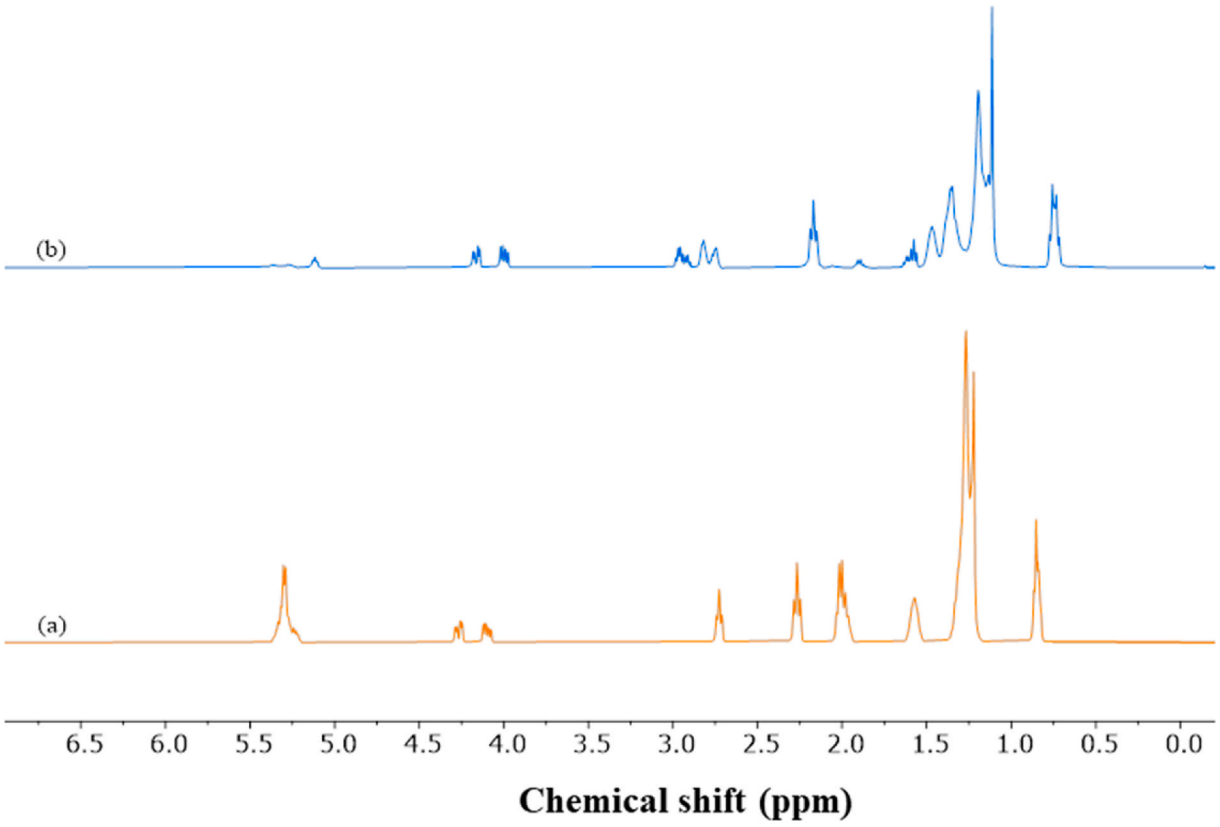

Fig. 9. ^{1}H -NMR spectrum of AMO (a) and EAMO (b).

Moreso, the removal of the ethylenic double bond in the AMO at 130 ppm (Fig. 10a) and the appearance of a new peak at 53–58 ppm (Fig. 10b) of ^{13}C NMR spectra of EAMO also indicated that the conversion of the ethylenic double bond in the AMO into EAMO.

3.7. Physicochemical characteristics of AMO and EAMO

Argemone mexicana oil (AMO) is remarkable a renewable resource for the epoxidation with peroxy acetic acid formed in situ using a heterogeneous solid acid catalyst. Thus, the physicochemical characteristics of AMO were examined as shown in Table 4. Moreover, the fatty acids content of AMO were 24.92% oleic acid (C18:1), 59.43% of Linolenic acid (C18:2), and 15.65% saturated fatty acids and contained an iodine value (IV) of 118.21 g I_2 per 100g of oil. AMO epoxide (EAMO) could be used to synthesize valuable goods such as plasticizers, lubricants, polymers, stabilizers, and others [3]. Thus, the physicochemical characteristics of epoxidized AMO were also examined and tabulated in Table 4. The amount of epoxide generated is dependent on the number of double bonds present in the oil, which is defined by the iodine value. The unsaturation of the raw material increased as the iodine value rises. When compared to AMO, the iodine value decreased from 118.21 to 5.62 g I_2/100g of AMO. This shows the conversion of unsaturation present in the AMO into its epoxidized form. The obtained flash point of EAMO was 280 °C. Thus, the epoxidized version of AMO can be utilized as a plasticizer in polymeric materials and as a high-temperature diesel fuel additive as a lubricant because it contains ether and ester functionality which enhances its compatibility [3]. The oxidative stability of AMO and EAMO was determined according to A Metrohm AG Rancimat model 892 (Herisau/Switzerland). It was used to assess the oxidative induction time (OIT) in accordance with AOCS Official Method Cd 12b-92, AOCS 1992. Thus, the oxidative induction time of the extracted AMO and its epoxidized oil (EAMO) was found to be 2.13 h and 68.41 h, respectively (Table 4 and Supplementary Fig. S1).

The viscosity of epoxidized products such as lubricants and plasticizers is critical to their lubricity. The viscosity of fluids decreases as temperature rises, and a measure called the viscosity index was employed to enumerate this trend. The greater the viscosity index value, the less the viscosity of the substance changes with temperature [3]. This work investigated the kinematic viscosities of AMO and its epoxidized oil (EAMO) at a temperature ranging from 20 to 100 °C (Fig. 11). It was revealed that the viscosity of both AMO and its epoxidized oil (EAMO) decreased with rises in the temperature. The kinematic viscosity of AMO was 31.05 mm^2/s at 40 °C and 5.56 mm^2/s at 100 °C, and its epoxidized form (EAMO) had a value increased to 131.5 mm^2/s at 40 °C and 7.26 at 100 °C (Table 4). The reason behind the increment of kinematic viscosity of EAMO was due to the ethylenic double bond in the AMO was removed through epoxidation. The kinematic viscosities of the present study were within the range of vegetable oil-based epoxy products such as lubricants (5–225 mm^2/s at 40 °C and 2–20 mm^2/s at 100 °C) [53]. The viscosity index of AMO decreased from 163.3 to 136.8 due to the disappearance of the double bond in the AMO. As a result, the viscosity and viscosity index of the EAMO falls within the given ranges, meeting the ISO VG 100 grade viscosity for industrial applications [53].

Fig. 11 depicts the trend of dynamic viscosity as a function of temperature for AMO and epoxidized AMO (EAMO). It was revealed from Fig. 11 that as the temperature increased the dynamic viscosity of both AMO and EAMO decreased. It was also shown in Fig. 11 that the dynamic viscosity of EAMO is much greater than AMO from 20 to 60 °C. The reason was due to the conversion of the double bond in the AMO to epoxide product, EAMO during in situ epoxidation.

3.8. Comparison of literature with the present study

Table 5 [7,18,24,54–57], depicts the comparison of literature with other heterogeneous metal oxide catalytic system for epoxidation of vegetable oils. The ethylenic double bond conversion of 89.7%, 75% and 96% were obtained from epoxidation of soybean oil using Ti–SiO_2 catalyst at reaction condition of 90 °C and 54 h [18], Alumina catalyst at reaction condition of 80 °C and 10 h [54] and HY zeolite catalyst at reaction condition of 70 °C and 3 h [56], respectively. Similarly, The ethylenic double bond conversion of 90% was obtained from Cardanol oil and Jatropha oil using Amberlite IR 120 at the catalyst loading of 20–22 wt%, and reaction condition of 65 °C, and 7 h. These results were in comparable to the present study as shown in Table 5.

4. Conclusion

Sulfated tin (IV) oxide solid acid catalyst was successfully synthesized and characterized in this study. Sulfated tin (IV) oxide solid acid was an effective catalyst for the epoxidation of AMO with peroxyacetic acid formed in situ. The maximum ethylenic double bond conversion of 95.5% with an epoxy oxygen content of 6.25 was obtained at the molar ratio of the ethylenic double bond in the AMO: H_2O_2, acetic acid was 1:2.5, 1:1.5, catalyst concentration 12.5% and reaction temperature at 343 k for 6 h. Epoxy group formation was confirmed using FT-IR, ^1H, and ^{13}C NMR spectroscopy. The physicochemical characteristics of EAMO indicate improved viscosity and oxidative stability, which leads to high lubricity when compared to its precursor, AMO. The catalyst and the AMO epoxide product were potential sources for PVC bioplasticizers synthesis.

Declarations and statements

Authors' contributions

1) Fekadu Ashine, Subramanian Balakrishnan, Zebene Kiflie, and Belachew Zegale Tizazu conceived and designed the experiments.
2) Fekadu Ashine performed the experiments.
3) Fekadu Ashine, Subramanian Balakrishnan, Zebene Kiflie, and Belachew Zegale Tizazu analyzed and interpreted the data.

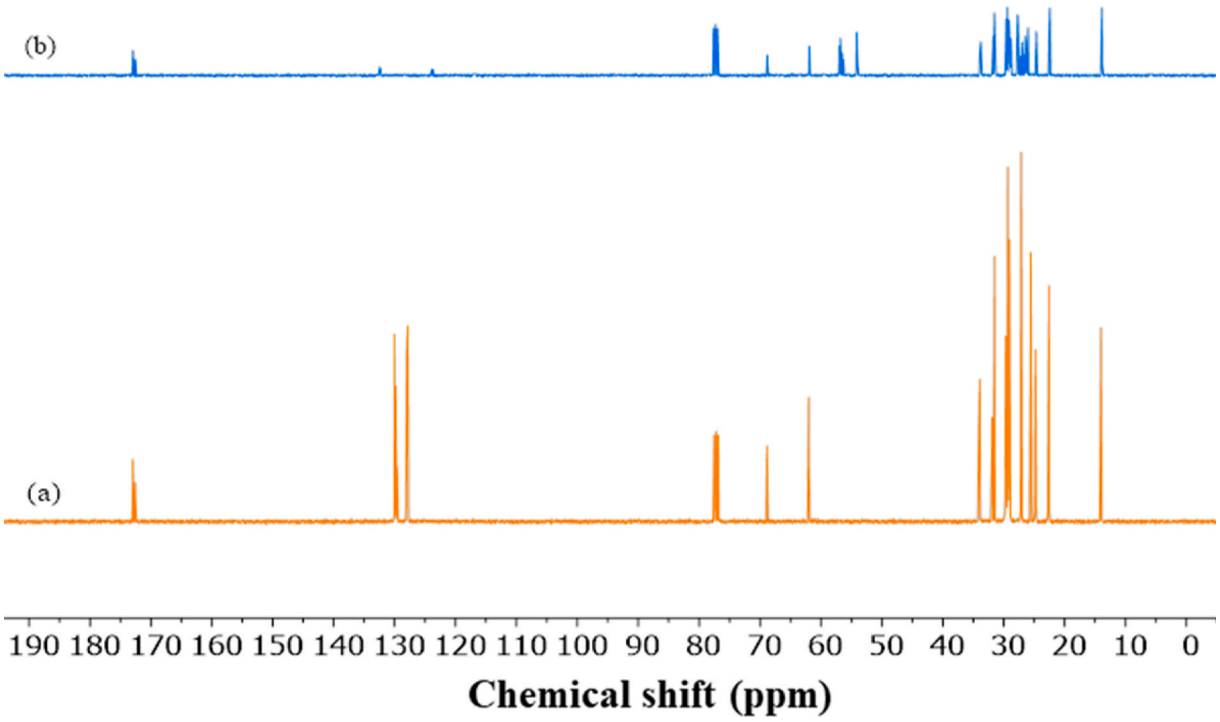

Fig. 10. ^{13}C NMR spectrum of AMO (a) and EAMO (b).

Table 4
Physicochemical characteristics of AMO and EAMO.

Characteristics	Unit	AMO	EAMO
Appearance	–	Dark brown	Slightly yellow viscous liquid
Density at 40 °C	kg/m^3	900 ± 1.34	976 ± 1.51
Kinematic viscosity at 40 °C	mm^2/s	31.05 ± 0.62	124.0 ± 0.74
Kinematic viscosity at 100 °C	mm^2/s	7.3 ± 0.07	18.8 ± 0.15
Viscosity index	–	163.3 ± 0.86	136.8 ± 0.79
Iodine value (IV)	g I_2/100 g oil	118.21 ± 0.52	7.7 ± 0.08
Epoxy oxygen content	–	–	6.25 ± 0.04
Flash point	°C	237 ± 1.03	280 ± 1.36
Induction period	h	2.13	68.41

4) Fekadu Ashine, Subramanian Balakrishnan, Zebene Kiflie, and Belachew Zegale Tizazu contributed reagents, materials, analysis tools or data.

5) Fekadu Ashine, Subramanian Balakrishnan, Zebene Kiflie, and Belachew Zegale Tizazu wrote the paper.

Funding

No funding was received to assist with the preparation of this manuscript.

Conflicts of interest

We do not have any conflict of interest.

Ethics approval and consent to participate

All authors mutually agreed that the manuscript to be submitted to the Heliyon Journal and the work has not been published/ submitted or is being submitted to another journal.

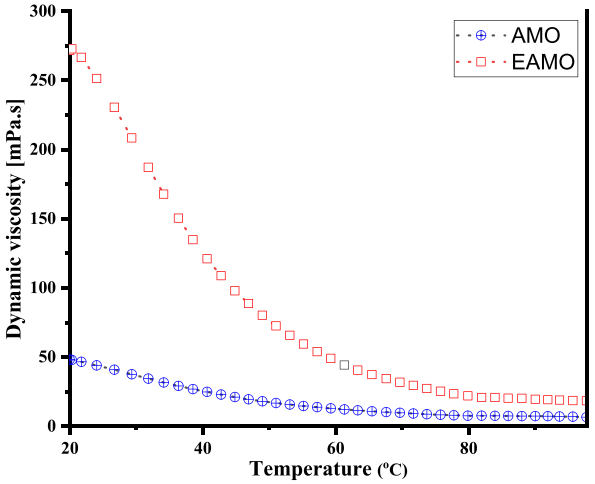

Fig. 11. Dynamic viscosity of AMO and EAMO at a constant shear rate of 50 s^{-1}.

Table 5
Comparison of literature with other heterogeneous metal oxide catalytic system for epoxidation of vegetable oils.

Feedstocks	Catalyst (wt %)	Oxidant	Reaction condition	EDB:H_2O_2:AA	% EDB conversion	References
Soybean oil	Ti–SiO_2 (6)	TBA	90 °C, 54 h,	1:1.1	89.7	[18]
Castor oil	Amberlite IR-120 (15)	Peracetic acid	50 °C, 8 h.	1:1.5:0.5	78.32	[7]
Soybean oil	Alumina	–	80 °C, 10 h	1:4	75	[54]
Rapeseed oil	Nb–SiO_2	–	90 °C, 4 h, 800 rpm	1:4	44	[55]
Soybean oil	HY zeolite (6)	Performic acid	70 °C, 3 h	1:1.5:0.18	96%	[56]
Cardanol oil	Amberlite IR 120 (22)	Peracetic acid	65 °C, 7 h,	1:1.5:0.5	90	[24]
Jatropha oil	Amberlite IR-120 (20)	Peracetic acid	–	–	90	[57]
Argemone Mexican oil	Sulfated tin (IV) oxide (12.5)	Peracetic acid	70 °C, 6 h, 1000 rpm	1:2.5:2	95.5	**This study**

EDB = Ethylenic double bond, AA = Acetic acid, TBA = Tertbutyl-alcohol, Nb–SiO_2–niobium–silica.

Availability of data and materials

The datasets generated during and/or analyzed during the current study are available from the corresponding author upon reasonable request.

Consent for publication

We request you to kindly consider our manuscript for possible publication in your esteemed journal.

Acknowledgment

The authors would like to thank Addis Ababa Science and Technology University and Chemical and Construction Inputs Industry Development Institute to allow experimental set-up work and analytical instruments for characterization.

Appendix A. Supplementary data

Supplementary data related to this article can be found at https://doi.org/10.1016/j.heliyon.2023.e12817.

References

[1] R. Turco, R. Tesser, M.E. Cucciolito, M. Fagnano, L. Ottaiano, S. Mallardo, M. Di Serio, Cynara cardunculus biomass recovery: an eco-sustainable, nonedible resource of vegetable oil for the production of poly (lactic acid) bioplasticizers, ACS Sustainable Chem. Eng. 7 (4) (2019) 4069–4077, https://doi.org/10.1021/acssuschemeng.8b05519.

[2] X. Pan, P. Sengupta, D.C. Webster, Novel biobased epoxy compounds: epoxidized sucrose esters of fatty acids, Green Chem. 13 (4) (2011) 965–975, https://doi.org/10.1039/c8gc03857k.

[3] A.K. Somidi, R.V. Sharma, A.K. Dalai, Synthesis of epoxidized canola oil using a sulfated-sno2 catalyst, Ind. Eng. Chem. 53 (49) (2014) 18668–18677, https://doi.org/10.1021/ie500493m.

[4] G. Karmakar, P. Ghosh, K. Kohli, B.K. Sharma, S.Z. Erhan, Chemicals from vegetable oils, fatty derivatives, and plant biomass, Innov. Uses Agric. Prod. Byproducts (2020) 1–31.

[5] R. Becker, A. Knorr, An evaluation of antioxidants for vegetable oils at elevated temperatures, Lubric. Sci. 8 (2) (1996) 95–117, https://doi.org/10.1002/ls.3010080202.

[6] Z. Lozada, G.J. Suppes, Y.C. Tu, F.H. Hsieh, Soy-based polyols from oxirane ring opening by alcoholysis reaction, Appl. Polym. 113 (4) (2009) 2552–2560, https://doi.org/10.1002/app.30209.

[7] S. Sinadinović-Fišer, M. Janković, O. Borota, Epoxidation of castor oil with peracetic acid formed in situ in the presence of an ion exchange resin, Chem. Eng. Process 62 (2012) 106–113, https://doi.org/10.1016/j.cep.2012.08.005.

[8] M.J. Snež ana Sinadinovic′ Fišer, Olga Borota, Epoxidation of castor oil with peracetic acid formed in situ in the presence of an ion exchange resin, Chem. Eng. Process 62 (2012) 106–113.

[9] A.S.A. Hazmi, M.M. Aung, L.C. Abdullah, M.Z. Salleh, M.H. Mahmood, Producing jatropha oil-based polyol via epoxidation and ring opening, Ind. Crop. Prod. 50 (2013) 563–567, https://doi.org/10.1016/j.indcrop.2013.08.003.

[10] S. Dinda, A.V. Patwardhan, V.V. Goud, N.C. Pradhan, Epoxidation of cottonseed oil by aqueous hydrogen peroxide catalysed by liquid inorganic acids, Bioresour. Technol. 99 (9) (2008) 3737–3744, https://doi.org/10.1016/j.biortech.2007.07.015.

[11] V.V. Goud, A.V. Patwardhan, N.C. Pradhan, Studies on the epoxidation of mahua oil (madhumica indica) by hydrogen peroxide, Bioresour. Technol. 97 (12) (2006) 1365–1371, https://doi.org/10.1016/j.biortech.2005.07.004.

[12] P.T. Wai, P. Jiang, Y. Shen, P. Zhang, Q. Gu, Y. Leng, Catalytic developments in the epoxidation of vegetable oils and the analysis methods of epoxidized products, RSC Adv. 9 (65) (2019) 38119–38136, https://doi.org/10.1039/c9ra05943a.

[13] G. Brahmachari, D. Gorai, R. Roy, Argemone mexicana: chemical and pharmacological aspects, Rev. Bras. Farmacogn. 23 (3) (2013) 559–567, https://doi.org/10.1590/S0102-695X2013005000021.

[14] A.A. Martínez-Delgado, J. de Anda, J.M. León-Morales, J.C. Mateos, A. Gutiérrez-Mora, J.J. Castañeda-Nava, Argemone species: potential source of biofuel and high-value biological active compounds, Environ. Eng. Res. (2021).

[15] J. Chen, M. de Liedekerke Beaufort, L. Gyurik, J. Dorresteijn, M. Otte, R.J.K. Gebbink, Highly efficient epoxidation of vegetable oils catalyzed by a manganese complex with hydrogen peroxide and acetic acid, Green Chem. 21 (9) (2019) 2436–2447, https://doi.org/10.1039/c8gc03857k.

[16] A. Overeem, G. Buisman, J. Derksen, F. Cuperus, L. Molhoek, W. Grisnich, C. Goemans, Seed oils rich in linolenic acid as renewable feedstock for environment-friendly crosslinkers in powder coatings, Ind. Crop. Prod. 10 (3) (1999) 157–165, https://doi.org/10.1016/S0926-6690(99)00018-7.

[17] M.J.H. Jalil, Abdul Azmi, Intan Suhada, Catalytic epoxidation of palm oleic acid using in situ generated performic acid–optimization and kinetic studies, Mater. Chem. Phys. 270 (2021), 124754.

[18] A. Campanella, M.A. Baltanas, M. Capel-Sanchez, J. Campos-Martin, J. Fierro, Soybean oil epoxidation with hydrogen peroxide using an amorphous ti/sio 2 catalyst, Green Chem. 6 (7) (2004) 330–334, https://doi.org/10.1039/B404975F.

[19] Z.S. Petrović, A. Zlatanić, C.C. Lava, S. Sinadinović-Fišer, Epoxidation of soybean oil in toluene with peroxoacetic and peroxoformic acids—kinetics and side reactions, Eur. J. Lipid Sci. Technol. 104 (5) (2002) 293–299, https://doi.org/10.1002/1438-9312, 200205)104:5<293::AID-EJLT293>3.0.CO;2-W.

[20] P.D. Jadhav, A.V. Patwardhan, R.D. Kulkarni, Kinetic study of in situ epoxidation of mustard oil, Mol. Catal. 511 (2021), 111748.

[21] H. Hosney, B. Nadiem, I. Ashour, I. Mustafa, A. El-Shibiny, Epoxidized vegetable oil and bio-based materials as pvc plasticizer, J. Appl. Polym. Sci. 135 (20) (2018), 46270, https://doi.org/10.1021/acssuschemeng.8b00884.

[22] J. Wang, X. Zhao, D. Liu, Preparation of epoxidized fatty acid methyl ester with in situ auto-catalyzed generation of performic acid and the influence of impurities on epoxidation, Waste Biomass Valoriza 9 (10) (2018) 1881–1891, https://doi.org/10.1007/s12649-017-9945-6.

[23] Y. Bai, J. Wang, D. Liu, X. Zhao, Conversion of fatty acid methyl ester to epoxy plasticizer by auto-catalyzed in situ formation of performic acid: kinetic modeling and application of the model, J. Clean. Prod. 259 (2020), 120791, https://doi.org/10.1016/j.jclepro.2020.120791.

[24] R. Mungroo, V.V. Goud, N.C. Pradhan, A.K. Dalai, Modification of epoxidised canola oil, Asia Pac. J. Chem. Eng. 6 (1) (2011) 14–22, https://doi.org/10.1002/apj.448.

[25] Lathi, Mattiasson, Green approach for the preparation of biodegradable lubricant base stock from epoxidized vegetable oil, Appl. Catal., B 69 (3–4) (2007) 207–212, https://doi.org/10.1016/j.apcatb.2006.06.016.

[26] T. Saurabh, M. Patnaik, S. Bhagt, V. Renge, Epoxidation of vegetable oils: a review, Int. J. Adv. Eng. Technol. 2 (4) (2011) 491–501.

[27] X. Zhang, J. Burchell, N.S. Mosier, Enzymatic epoxidation of high oleic soybean oil, ACS Sustainable Chem. Eng. 6 (7) (2018) 8578–8583, https://doi.org/10.1021/acssuschemeng.8b00884.

[28] T. Vlček, Z.S. Petrović, Optimization of the chemoenzymatic epoxidation of soybean oil, J. Am. Oil Chem. Soc. 83 (3) (2006) 247–252, https://doi.org/10.1007/s11746-006-1200-4.

[29] S. Sun, X. Ke, L. Cui, G. Yang, Y. Bi, F. Song, X. Xu, Enzymatic epoxidation of sapindus mukorossi seed oil by perstearic acid optimized using response surface methodology, Ind. Crop. Prod. 33 (3) (2011) 676–682, https://doi.org/10.1016/j.indcrop.2011.01.002.

[30] A.S. Bajwa, S. Sathaye, V.M. Kulkarni, A.V. Patwardhan, Chemoenzymatic epoxidation of karanja oil: an alternative to chemical epoxidation, Asia Pac. J. Chem. Eng. 11 (2) (2016) 314–322, https://doi.org/10.1002/apj.1979.

[31] A.Z. Fadhel, P. Pollet, C.L. Liotta, C.A. Eckert, Combining the benefits of homogeneous and heterogeneous catalysis with tunable solvents and nearcritical water, Molecules 15 (11) (2010) 8400–8424, https://doi.org/10.3390/molecules15118400.

[32] V.V. Goud, A.V. Patwardhan, S. Dinda, N.C. Pradhan, Epoxidation of karanja (pongamia glabra) oil catalysed by acidic ion exchange resin, Eur. J. Lipid Sci. Technol. 109 (6) (2007) 575–584, https://doi.org/10.1002/ejlt.200600298.

[33] H. Yuan, Z. Dong, J. He, Y. Wang, H. Zhang, Surface characterization of sulfated zirconia and its catalytic activity for epoxidation reaction of castor oil, Chem. Eng. Commun. 206 (12) (2019) 1618–1627, https://doi.org/10.1080/00986445.2018.1560274.

[34] Y.M. Bayisa, W.A. Teso, Solid sulfonated silica acid catalyst for epoxidation of podocarpus falcatus seed oil, Biomass Convers. Biorefin. (2021) 1–10.

[35] P.A. Suarez, M.S. Pereira, K.M. Doll, B.K. Sharma, S.Z. Erhan, Epoxidation of methyl oleate using heterogeneous catalyst, Ind. Eng. Chem. 48 (7) (2009) 3268–3270, https://doi.org/10.1021/ie801635b.

[36] M.T. Benaniba, N. Belhaneche-Bensemra, G. Gelbard, Kinetics of tungsten-catalyzed sunflower oil epoxidation studied by 1h nmr, Eur. J. Lipid Sci. Technol. 109 (12) (2007) 1186–1193, https://doi.org/10.1002/ejlt.200700114.

[37] R.V. Sharma, A.K. Dalai, Synthesis of bio-lubricant from epoxy canola oil using sulfated ti-sba-15 catalyst, Appl. Catal., B 142 (2013) 604–614, https://doi.org/10.1016/j.apcatb.2013.06.001.

[38] R. Varala, V. Narayana, S.R. Kulakarni, M. Khan, A. Alwarthan, S.F. Adil, Sulfated tin oxide (sto)–structural properties and application in catalysis: a review, Arab. J. Chem. 9 (4) (2016) 550–573, https://doi.org/10.1016/j.arabjc.2016.02.015.

[39] J.-L. Zheng, J. Wärnå, F. Burel, T. Salmi, B. Taouk, S. Leveneur, Kinetic modeling strategy for an exothermic multiphase reactor system: application to vegetable oils epoxidation by using Prileschajew method, AIChE J. 62 (3) (2016) 726–741.

[40] S. Leveneur, M. Pinchard, A. Rimbault, M. Safdari Shadloo, T. Meyer, Parameters affecting thermal risk through a kinetic model under adiabatic condition: application to liquid-liquid reaction system, Thermochim. Acta (2018) 10–17.

[41] X. Cai, J.-L. Zheng, A. Freites, L. AguileraVernières-Hassimi, P. Tolvanen, T. Salmi, S. Leveneur, Influence of ring opening reactions on the kinetics of bio-based cottonseed oil epoxidation, Int. J. Chem. Kinet. 50 (10) (2018) 726–741.

[42] A.S. Reshad, P. Tiwari, V.V. Goud, Extraction of oil from rubber seeds for biodiesel application: optimization of parameters, Fuel 150 (2015) 636–644, https://doi.org/10.1016/j.fuel.2015.02.058.

[43] A. Khder, E. El-Sharkawy, S. El-Hakam, A. Ahmed, Surface characterization and catalytic activity of sulfated tin oxide catalyst, Catal. Commun. 9 (5) (2008) 769–777, https://doi.org/10.1016/j.catcom.2007.08.022.

[44] M.L. Nejati, , Bafghi Karimabad Asalavati, Niasari Safardoust, Synthesis and characterization of sno2 nanostructures prepared by a facile precipitation method, J. Nanostruc. (2015), https://doi.org/10.7508/jns.2015.01.007.

[45] L. Yurkova, S. Lermontov, V. Kazachenko, V. Ivanov, A. Lermontov, A. Baranchikov, L. Vasil'Eva, Sulfated sno 2 as a high-performance catalyst for alkene oligomerization, Inorg. Mater. 48 (10) (2012) 1012–1019, https://doi.org/10.1134/S0020168512100147.
[46] M. Kurańska, H. Beneš, A. Prociak, O. Trhlíková, Z. Walterova, W. Stochlińska, Investigation of epoxidation of used cooking oils with homogeneous and heterogeneous catalysts, J. Clean. Prod. 236 (2019), 117615, https://doi.org/10.1016/j.jclepro.2019.117615.
[47] V.V. Goud, A.V. Patwardhan, S. Dinda, N.C. Pradhan, Kinetics of epoxidation of jatropha oil with peroxyacetic and peroxyformic acid catalysed by acidic ion exchange resin, Chem. Eng. Sci. 62 (15) (2007) 4065–4076, https://doi.org/10.1016/j.ces.2007.04.038.
[48] C.M. Agu, K. Nwosu-Obieogu, K.A. Ani, A.C. Agulanna, S.O. Iwu-Ejike, O.O. Oguegbu, M.C. Menkiti, Chemical modification of Terminalia catappa L. kernel oil methyl ester using epoxidation-esterification approach, for application as bio-transformer fluid–Physicochemical characterization, kinetics and thermodynamics, Clean. Chem. Engin. 3 (2022), 100035.
[49] M.J. Jalil, A.F.M. Yamin, I.S. Azmi, S.K. Jamaludin, A.R.M. Daud, Mechanism and kinetics study in homogenous epoxidation of vegetable oil, Int. J. Eng. Technol. 7 (4.42) (2018) 124–126.
[50] S. Cai, L. Wang, Epoxidation of unsaturated fatty acid methyl esters in the presence of SO3H-functional brønsted acidic ionic liquid as catalyst, Chin. J. Chem. Eng. 19 (1) (2011) 57–63.
[51] C. Cai, H. Dai, R. Chen, C. Su, X. Xu, S. Zhang, L. Yang, Studies on the kinetics of in situ epoxidation of vegetable oils, Eur. J. Lipid Sci. Technol. 110 (4) (2008) 341–346.
[52] B. Lin, L. Yang, H. Dai, A. Yi, Kinetic studies on oxirane cleavage of epoxidized soybean oil by methanol and characterization of polyols, J. Am. Oil Chem. Soc. 85 (2) (2008) 113–117.
[53] M.C. Hernández-Cruza, R.M. G, Z. Domínguezb, A. Rosales-Quinteroa, M. Abud-Archilaa, T. Ayora-Talaverac, J.J. Villalobos-Maldonadoa, Optimization and characterization of in situ epoxidation of chicken fat with peracetic acid, Fuel 285 (2021) 119127, https://doi.org/10.1016/j.fuel.2020.119127.
[54] R. Turco, C. Pischetola, R. Tesser, S. Andini, M. Di Serio, New findings on soybean and methylester epoxidation with alumina as the catalyst, RSC Adv. 6 (38) (2016) 31647–31652.
[55] S. Dworakowska, C. Tiozzo, M. Niemczyk-Wrzeszcz, P. Michorczyk, N. Ravasio, R. Psaro, M. Guidotti, Mesoporous molecular sieves containing niobium (v) as catalysts for the epoxidation of fatty acid methyl esters and rapeseed oil, J. Clean. Prod. 166 (2017) 901–909.
[56] R. Turco, C. Pischetola, M. Di Serio, R. Vitiello, R. Tesser, E. Santacesaria, Selective epoxidation of soybean oil in the presence of h–y zeolite, Ind. Eng. Chem. Res. 56 (28) (2017) 7930–7936.
[57] L.A. Rios, D.A. Echeverri, A. Franco, Epoxidation of jatropha oil using heterogeneous catalysts suitable for the prileschajew reaction: acidic resins and immobilized lipase, Appl. Catal. Gen. 394 (1–2) (2011) 132–137.